

hydrous silicic melts (20). Relative to oxygen fugacity, pressure and temperature are less important in controlling the magnitude of the partition coefficients. In a series of experiments where oxygen fugacity was 0.5 log units above the Ni-NiO buffer, *D* ranged from 47 to 137 at 0.5 to 3 kbar and 750° to 850°C. Similarly, changing the alkali/aluminum ratio or adding small amounts of CaO or FeO did not change the order of magnitude of the partition coefficients. However, larger concentrations of CaO or FeO may stabilize sulfur-bearing minerals (17) or immiscible sulfide melts.

Explosive volcanic activity requires the presence of a free fluid phase. Under conditions slightly above the Ni-NiO buffer (with *D* ranging from 47 to 137), 2 weight % or less fluid in the magma chamber will be sufficient to extract half of the total mass of sulfur out of the entire magma reservoir. Because the mass of erupted magma is usually only a fraction of the total melt stored in the magma chamber (1, 21), it is not surprising that huge amounts of excess sulfur are observed upon eruption. Under reducing conditions, where H₂S is the major sulfur species in the fluid, the extraction of sulfur becomes even more efficient; however, such reducing conditions are probably unlikely to prevail in the subduction zone setting of most explosive volcanoes (1–7).

The principles outlined above can be illustrated using some data from the 1991 Mount Pinatubo eruption. The Pinatubo magma contained 60 to 90 ppm of sulfur, was relatively oxidized (between the Ni-NiO and hematite-magnetite buffers), and originated from a magma chamber with a confining pressure around 2 kbar and a temperature around 780°C (1–3 and references therein). Accordingly, *D* should be close to 47. This would mean that the fluid phase in equilibrium with the hydrous melt in the magma chamber should have contained between 0.56 and 0.85 weight % SO₂. To account for the estimated 17 megatons of SO₂ released would require 8 to 25 weight % of free fluid in the erupted magma that produced 5 to 10 km³ of pyroclastic deposits. This number appears relatively large; however, seismic evidence suggests the presence of a magma chamber containing 40 to 90 km³ of melt below Mount Pinatubo (21). Relative to the entire reservoir of melt in this chamber, the free fluid phase released upon eruption would only amount to 0.9 to 3 weight %. If one assumed such a small fraction of hydrous fluid to be present in the magma chamber before eruption, a sulfur partition coefficient of 47 would imply that 30 to 59% of the total sulfur in the entire magma chamber is concentrated in the fluid, provided that the fluid has reached equilibrium with the entire reservoir. This is possible if one assumes an upward accumulation of fluid over long periods into shallower parts of the magma chamber, as suggested by Gerlach *et al.* (1). If the original sulfur content in the melt had been

90 ppm, the highest value found in melt inclusions (2), this would amount to a total mass of 5 to 24 megatons of SO₂ extracted by the fluid, consistent with the estimate of 17 megatons released upon eruption.

The calculations presented above emphasize the importance of considering the amount of sulfur stored in the entire magma chamber in estimating the sulfur released in explosive volcanism. Estimates based on the sulfur content of the erupted melt alone would severely underestimate the environmental impact of explosive volcanism in the geologic past.

References and Notes

1. T. M. Gerlach, H. R. Westrich, R. B. Symonds, in *Fire and Mud: Eruptions and Lahars of Mount Pinatubo, Philippines*, C. G. Newhall and R. S. Punongbayan, Eds. (Univ. of Washington Press, Seattle, 1996), pp. 415–433.
2. P. J. Wallace and T. M. Gerlach, *Science* **265**, 497 (1994).
3. V. Kress, *Nature* **389**, 591 (1997).
4. T. M. Gerlach and K. A. McGee, *Geophys. Res. Lett.* **21**, 2833 (1994).
5. J. F. Luhr, I. S. Carmichael, J. C. Varekamp, *J. Volcanol. Geotherm. Res.* **23**, 69 (1984).
6. H. Sigurdson, S. Carey, J. M. Palais, J. Devine, *ibid.* **41**, 127 (1990).
7. T. M. Gerlach, H. R. Westrich, T. J. Casadevall, D. L. Finnegan, *ibid.* **62**, 317 (1994).

8. G. J. S. Bluth, C. C. Schnetzler, A. J. Krueger, L. S. Walter, *Nature* **366**, 327 (1993).
9. M. P. McCormick, L. W. Thomason, C. R. Trepte, *ibid.* **373**, 399 (1995).
10. K. R. Briffa, P. D. Jones, F. H. Schweingruber, T. J. Osborn, *ibid.* **393**, 450 (1998).
11. D. M. Pyle, *ibid.*, p. 415.
12. M. R. Rampino and S. Self, *ibid.* **359**, 50 (1992).
13. S. Bekki *et al.*, *Geophys. Res. Lett.* **23**, 2669 (1996).
14. J. D. Devine, H. Sigurdsson, A. N. Davis, S. Self, *J. Geophys. Res.* **89**, 6309 (1994).
15. C. Oppenheimer, *Geophys. Res. Lett.* **23**, 2057 (1996).
16. S. N. Williams *et al.*, *J. Volcanol. Geotherm. Res.* **42**, 53 (1990).
17. B. Scaillet, B. Clemente, B. W. Evans, M. Pichavant, *J. Geophys. Res.* **103**, 23937 (1998).
18. I. M. Chou, *Am. J. Sci.* **286**, 638 (1986).
19. Cameca SX 50 with operating conditions of 20 KV acceleration voltage, 50 nA beam current, ZnS and BaSO₄ standard.
20. M. R. Carroll and M. J. Rutherford, *Am. Mineral.* **73**, 845 (1988).
21. J. Mori, D. Eberhart-Phillips, D. Harlow, *Eos* **74** (fall meeting suppl.), 667 (1993).
22. I thank D. Krause for carrying out all microprobe analyses presented in this study, A. Dietel and S. Lauterbach for analyses by inductively coupled plasma atomic emission spectrometry, and H. Schulze for sample preparation. I. Kravchuk performed some preliminary, unpublished experiments related to this study. Supported by the German Science Foundation (DFG) priority program on element partitioning.

20 January 1999; accepted 19 April 1999

A Mid-European Decadal Isotope-Climature Record from 15,500 to 5000 Years B.P.

Ulrich von Grafenstein,^{1*} Helmut Erlenkeuser,² Achim Brauer,³ Jean Jouzel,¹ Sigfus J. Johnsen⁴

Oxygen-isotope ratios of precipitation (δ¹⁸O_p) inferred from deep-lake ostracods from the Ammersee (southern Germany) provide a climate record with decadal resolution. The record in detail shows many of the rapid climate shifts seen in central Greenland ice cores between 15,000 and 5000 years before the present (B.P.). Negative excursions in the estimated δ¹⁸O_p from both of these records likely reflect short weakenings of the thermohaline circulation caused by episodic discharges of continental freshwater into the North Atlantic. Deviating millennial-scale trends, however, indicate that climate gradients between Europe and Greenland changed systematically, reflecting a gradual rearrangement of North Atlantic circulation during deglaciation.

The Greenland ice cores show strong quasi-periodic climatic oscillations during the longer term interglacial-glacial and glacial-inter-

glacial transitions. These Dansgaard-Oeschger events (DOEs) (1) are characterized by rapid warmings of almost glacial-interglacial amplitudes within decades, followed by some 2000 to 3000 years of gradual cooling, and a final cold phase of about 1000 years' duration, often with a weak, positive internal trend. Similar features have been found for Europe in long continental records of vegetation and magnetic sediment properties (2), as well as in marine proxy records (3). Modeling studies and data provide support for two alternative mechanisms: (i) triggering by oscillations of the northern hemispheric ice sheets (3) or (ii) oceanic oscillations without

¹Laboratoire des Sciences du Climat et de l'Environnement (LSCE), F-91198 Gif-sur-Yvette, France. ²Leibniz-Labor für Altersbestimmung und Isotopenforschung der Universität Kiel, Germany. ³Laboratoire de Botanique Historique et Palynologie, Faculté des Sciences et Techniques de Saint-Jerome, Marseille, France, and ⁴Geoforschungszentrum Potsdam, Germany. ⁵Department of Geophysics, University of Copenhagen, Copenhagen, Denmark, and Science Institute, University of Iceland, Reykjavik, Iceland.

*To whom correspondence should be addressed. E-mail: uligraf@lsce.cnrs-gif.fr

REPORTS

or with only weak external triggering (4). Here we present a detailed quantitative estimation of $\delta^{18}\text{O}_p$ in mid-Europe (from Ammersee, Germany) for the time period from 15,000 to 5000 years before the present, including the youngest of these DOEs. The new record, in which each analysis comprises ~ 11 years, permits comparison of European and Greenland climate during this period based on the same proxy and with almost identical temporal resolution and precision.

The Ammersee is a hard-water lake 20 km long and 81 m deep and is situated about 50 km southwest of Munich. The modern isotope hydrology of the lake is such that the oxygen isotopic composition of lake water ($\delta^{18}\text{O}_L$) is simply linked to the oxygen isotopic composition of precipitation ($\delta^{18}\text{O}_p$) (5). Even extreme hydrological shifts, such as a 50% decrease or increase in the input into the lake or in evaporation from the lake's surface, would change the observed offset between $\delta^{18}\text{O}_L$ and $\delta^{18}\text{O}_p$ (0.75‰) only by $\pm 0.38\%$. The $\delta^{18}\text{O}$ of ostracod shells from the profundal Ammersee can be used as direct tracer for $\delta^{18}\text{O}_L$. Water temperatures below 50-m water depth were probably close to 4°C throughout the lake's history. The temperature-dependent fractionation between calcite and water ($\sim -0.25\text{‰/K}$) can therefore be considered as constant. Vital offsets for $\delta^{18}\text{O}$ of the used species are known (6). A 200-year record of $\delta^{18}\text{O}_p$ from ostracods from this lake is well correlated with 200 years of mean air temperatures from the Hohenpeißenberg observatory in the watershed of the Ammersee. The inferred temporal $\delta^{18}\text{O}_p$ -temperature gradient for this period is 0.58 ‰/°C (5), almost identical to the interannual temperature sensitivity of $\delta^{18}\text{O}_p$ in Europe as derived from three decades of direct measurements (0.6 ‰/°C) (7).

$\delta^{18}\text{O}$ records of lake marls (8, 9) and of

benthic ostracods (10–12) in Europe, including littoral and sublittoral cores from the Ammersee (13, 14), have provided qualitative evidence for contemporaneous variations in $\delta^{18}\text{O}_p$ of Greenland and Europe during the Late Glacial. However, extracting $\delta^{18}\text{O}_p$ from such records has been impeded by secondary hydrological, water-temperature, and archive-specific effects and by their low temporal resolution (usually considerably more than 100 years per sample).

We analyzed data from two new cores from the Ammersee collected at 70-m water depth (AS96-1 and AS93-1). Together with the record from core AS92-5 (15), these new data provide an almost continuous $\delta^{18}\text{O}_L$ record for the period from 15,500 to 5500 yr B.P. (Fig. 1) at a temporal resolution of ~ 11 years. We infer $\delta^{18}\text{O}_p$ from $\delta^{18}\text{O}_L$ by correcting for the observed present-day difference of -0.75% , assuming that variations of the drainage-basin water balance (precipitation minus evapotranspiration) and of the long-term humidity have only negligible effect.

Within the sample resolution, the three major isotope shifts in AS96-1 match the major lithological changes. These changes are also seen in the shallow-water cores, and we thus used them to correlate the record with the regional pollen assemblage zones. The youngest part of the Ammersee $\delta^{18}\text{O}_p$ record (AS92-5, 8500 to 5000 cal. yr B.P.) has been correlated to the GRIP $\delta^{18}\text{O}_{ice}$ record with four ^{14}C measurements of macro remains (15). The new records also reproduce in great detail the GRIP $\delta^{18}\text{O}$ variations, if we account for the different offsets of the depth scales and the generally lower sedimentation rates at sites AS93-1 and AS96-1 (Fig. 1). The clearly visible common features (the rapid transitions as well as the N-shaped

early-Holocene event and the 8.2-ky event; solid lines in Fig. 1) and one ^{14}C date ($11,580 \pm 100$ ^{14}C -yr B.P., at 1167.25-cm core depth) were used as tie points for an initial age model. This corrects for the major changes of accumulation rates, expected as a result of observed lithological changes. Linear interpolation of the sample ages between these tie points is sufficient to achieve agreement within ~ 100 years of even very small $\delta^{18}\text{O}$ shifts (dashed lines in Fig. 1). Wiggle matching only was used to provide a final match, likely compensating moderate variations of sedimentation rates within the lithological units.

We tested this age model (GRIP-AS) by developing a second independent chronology for the AS96-1 record. The low- $\delta^{18}\text{O}$ events in the Ammersee record were matched to the Late Glacial cold phases as determined by lithological and palynological signals in a varved record from Lake Meerfelder Maar (MFM), situated about 500 km northwest of Ammersee (16). The Laacher See Tephra (12,880 yr B.P.) was used as an additional control point. The resulting depth-age functions (Fig. 2) confirm the reliability of our age model. Age differences between GRIP-AS and MFM-AS only exceed 150 years close to the base and top of the MFM chronology, where significant climate events are rare.

The Ammersee and GRIP $\delta^{18}\text{O}_p$ records were transformed into contemporaneous 10-year averages. Adjusting the records to the respective modern $\delta^{18}\text{O}_p$ values and expanding the European scale by the slope (1.5) of the linear regression ($R^2 = 0.85$) illustrates (i) that the correlation on centennial times scales might be even higher and (ii) that the records on millennial scale systematically deviate from the overall linear correlation (Fig. 3). The high similarity of short-term climate events, despite

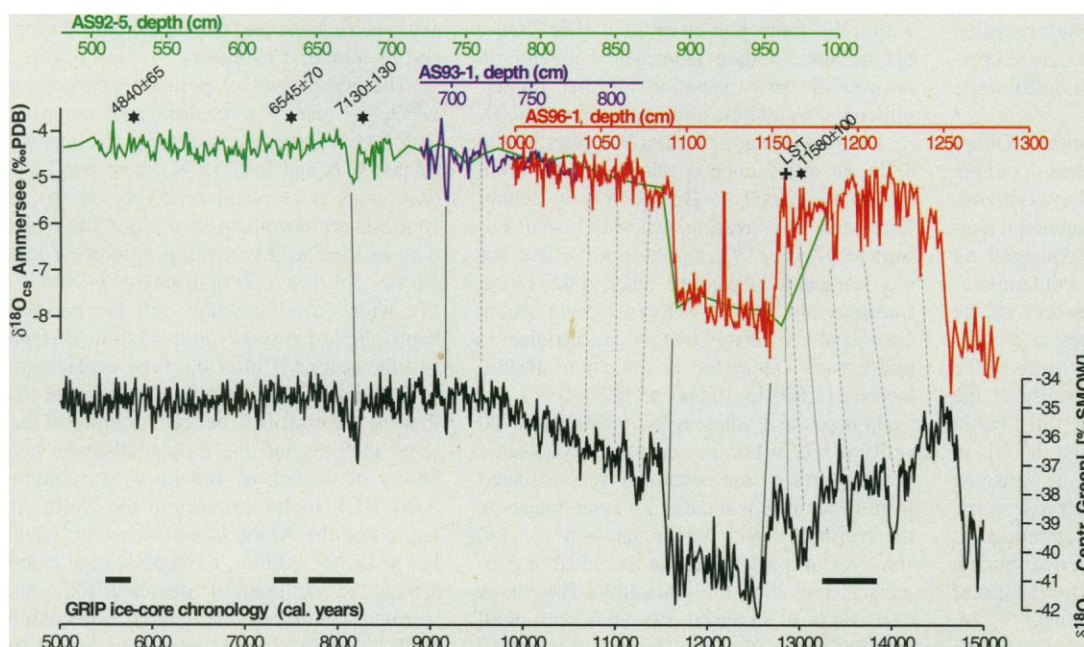
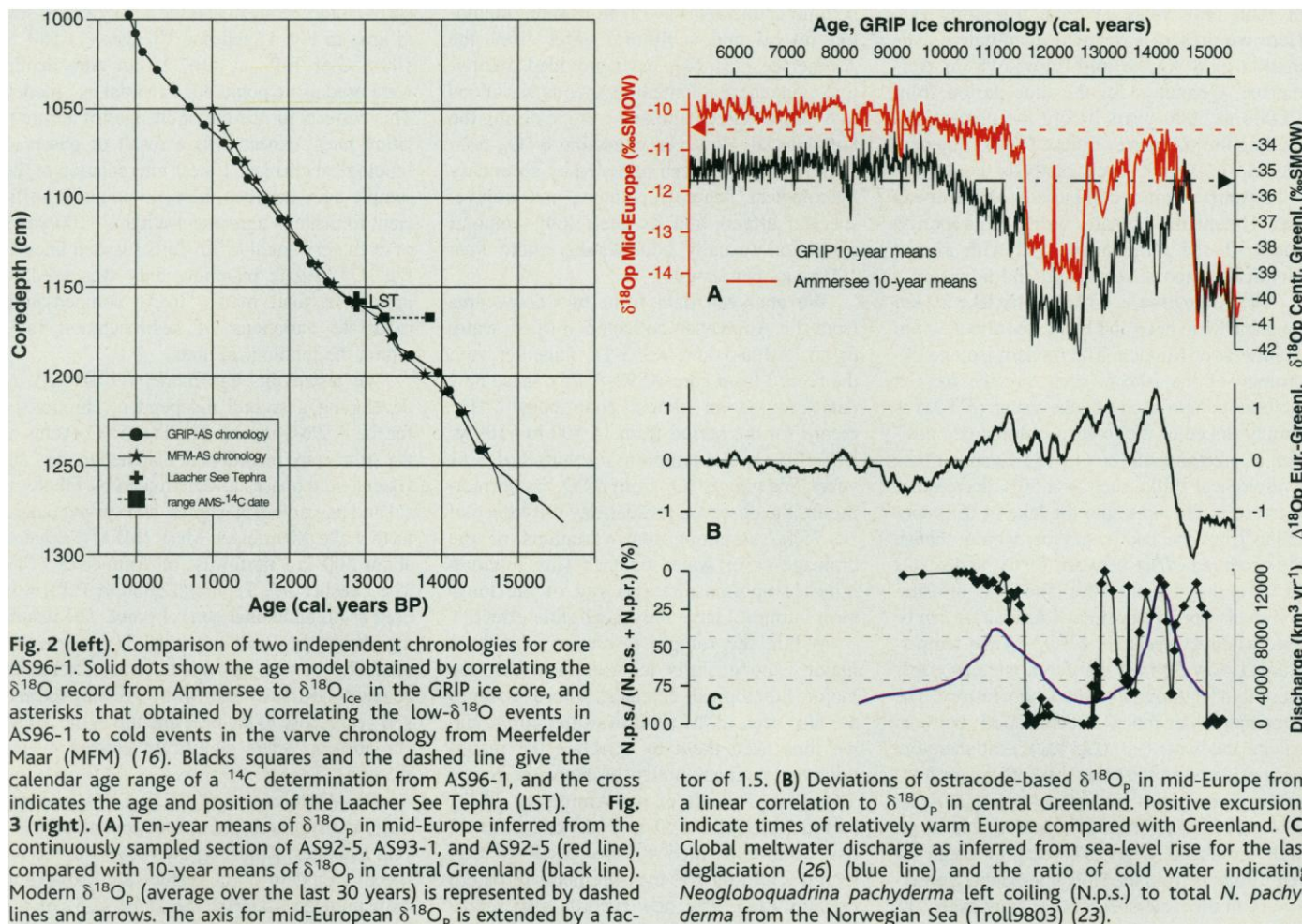


Fig. 1. (Top graphs) Oxygen isotope values of calcite shells of *Candona* sp. (juveniles of *Fabaeformiscandona levanderi* and *Fabaeformiscandona tricatricosa*) from sediment cores AS92-5 (green) (15), AS93-1 (blue), and AS96-1 (red); see (33) for further sampling details and isotope measurements. Asterisks and tilted labels indicate available ^{14}C dates; black bars denote the possible range of respective calendar years. (Lower graph) $\delta^{18}\text{O}$ ice record from Summit Greenland (GRIP) in a 10-year resolution based on the age model ss08c. Solid and dashed lines point to correlative events in both records.



the important differences of the respective boundary conditions and the possible moisture sources for the sites, suggests that both records mainly reflect air temperatures. A comparison of glacial to modern air-temperature differences for a number of atmospheric general circulation models also shows a 1.5 times stronger temperature change in Greenland than in mid-Europe (17).

The common rapid transitions Oldest Dryas–Bølling (OstD–Bø), Allerød–Younger Dryas (All–YD), and Younger Dryas–Preboreal (YD–PB), and the smaller centennial negative excursions can only be explained by climatic changes that occurred contemporaneously in both regions. Probably they are the local expression of rapid changes of the Atlantic northward heat transport by way of the salt conveyor-belt system. The cause of the centennial negative excursions, all within longer phases of relatively high $\delta^{18}\text{O}_p$ in Greenland and Europe, could be episodic short outbursts of large freshwater reservoirs, forming at the borders of the retreating ice sheets in Europe and North America. Such a mechanism is likely responsible for the last of these excursions (the 8.2-ky event) (15, 18, 19) and also was proposed for the Gerzensee

and PB oscillations (20). Evidently, such outburst events were too short to result in a longer term reorganization of the North Atlantic circulation. Similar events might have been part of the centennial-scale variability within the warm phases of the earlier DOEs, but because of their stochastic behavior do not provide an explanation for such regular millennial oscillations, including Bø–All–YD.

During OstD and the first 300 years of Bø, $\delta^{18}\text{O}_p$ in mid-Europe is relatively low. From 14,400 to 12,600 yr B.P., $\delta^{18}\text{O}_p$ in central Greenland is decreasing, whereas in mid-Europe long-term $\delta^{18}\text{O}_p$ seems more or less stable, leading to a positive relative difference. Consequently, the All–YD transition in central Greenland is relatively less pronounced than in mid-Europe. During the earliest part of the Holocene (11,600 to 10,000 yr B.P.) $\Delta^{18}\text{O}_{\text{Eu-Gr}}$ again is positive, whereas from 10,000 to 8700 yr BP $\delta^{18}\text{O}_p$ in Europe was relatively lower.

Sea-surface temperatures reconstructed from foraminifera and diatom assemblages in the North Sea and Norwegian Sea (21–23) show features similar to the record from Ammersee, including the plateau-like Bø–All. A decrease in $\delta^{18}\text{O}$ during Bø–All is seen in all deep-ice cores from the Greenland ice sheet

(24). Although other than regional temperature variations could have contributed to the observed relative differences of $\delta^{18}\text{O}_p$ between Europe and GRIP (25), we consider $\Delta^{18}\text{O}_{\text{Eu-Gr}}$ as a valid proxy for the climatic asymmetry between Greenland and Europe and its temporal evolution.

The two periods of positive excursions of $\Delta^{18}\text{O}_{\text{Eu-Gr}}$ (central Greenland cold compared with Europe) coincide with the global meltwater pulses Ia and Ib (26). Negative $\Delta^{18}\text{O}_{\text{Eu-Gr}}$ excursions (Greenland relatively warm), in contrast, are dominant in periods for which we can assume that melting rates were low; the first follows iceberg discharge event HE1 (3), which most probably left the northern hemispheric ice sheets in a subcritical stage, and the second is after the final deglaciation of Scandinavia. We therefore hypothesize that there is a causal link between long-term ice-sheet melting and the millennial-scale variability of Greenland and European climate. After HE1, meltwater flux to the North Atlantic and the Arctic Ocean was low, which led to higher salinity, reduced sea-ice extent around the southeastern Greenland coast, and warmer conditions in central Greenland. With the onset of deep-water formation in the

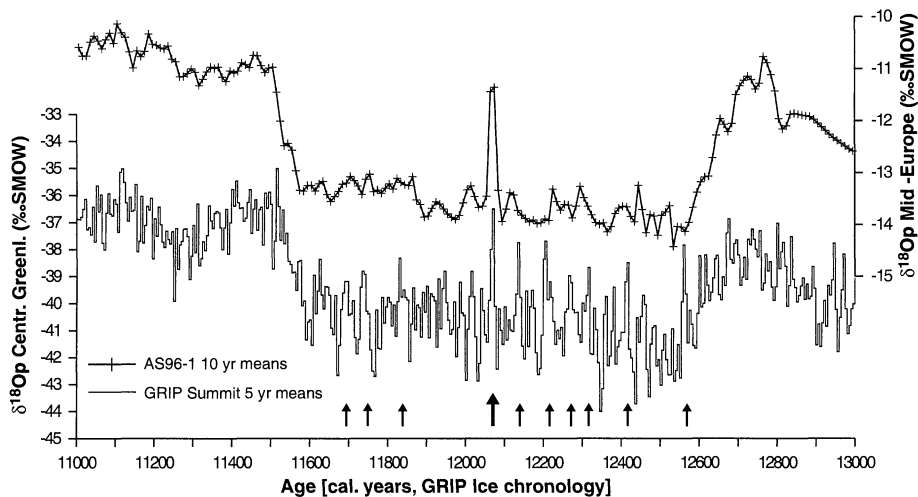


Fig. 4. The 5-year $\delta^{18}\text{O}_p$ record from Summit (lower graph) shows significantly higher variability during Younger Dryas than during Allerød and Preboreal. Short subdecadal positive excursions reach almost Holocene levels (arrows). In the European record (upper graph), only the highest and longest of these warm spikes is preserved, most likely as a result of high accumulation of detrital material, induced by the warm event itself by destabilizing frozen soils.

Norwegian Greenland Sea at the OstD-Bø transition, considerable parts of the surrounding ice sheets started to melt, thus increasing the meltwater discharge into the Nordic seas and enhancing the export of low-salinity water and ice through the Fram and Denmark straits. We assume that this process successively induced a broadening of the seasonal sea-ice belt around Greenland, leading to the long-term cooling trend during Bø-All in central Greenland, whereas Europe remained relatively warm until the east- and southward-moving polar front closed off the Iceland-Faroe strait and forced the deep-water formation to take place farther south. Such a switch-off of heat transport to the Norwegian sea would explain the rapid decrease of $\delta^{18}\text{O}_p$ at the beginning of YD in both Europe and Greenland, and the relatively stronger isotopic reaction in Europe.

For the 1500 years after the end of YD we assume that a similar meltwater feedback operated as during Bø-All, although more limited because of the final Scandinavian deglaciation. Between 10,000 to 8500 yr B.P. central Greenland was relatively warm, probably because the East Greenland current was less extensive (27–29).

Both transitions from cold to warm (OstD-Bø and YD-PB) were rapid [for example, less than 30 years in GRIP for YD-PB, and most within 10 years (30)], indicating that the climate system changes more easily into its warm mode. In addition, the 5-year resolution of $\delta^{18}\text{O}_p$ in the GRIP ice core shows several short positive excursions to almost Holocene values, confirming reduced climate stability during YD (Fig. 4, small arrows). In the Ammersee record such short-lived excursions are below the time resolution. However the strongest of the excursions of $\delta^{18}\text{O}_p$ in the GRIP record coincides

with the short positive excursion in the Ammersee record (Fig. 4, large arrow). The YD-type thermohaline circulation at this time probably was less stable owing to a short outburst of warm North Atlantic water into a Norwegian Greenland Sea covered with sea-ice, a mechanism that also could apply for the final termination of YD.

The proposed meltwater feedback mechanism for the gradual cooling into the YD might also explain the DOEs. In such an extended scenario, the smaller and more reactive Scandinavian ice sheet would be responsible for the occurrence intervals of DOEs (2000 to 3000 years) (31). The more inert Laurentide Ice Sheet, by growing more or less continuously during a certain number of such DOEs, would progressively reduce their amplitudes, until finally collapsing into a massive iceberg discharge (Heinrich Event) at the end of such longer term cooling cycles (Bond Cycles, 7000 to 10,000 years) (31, 32).

References and Notes

1. S. J. Johnsen *et al.*, *Nature* **359**, 311 (1992).
2. N. Thouveny *et al.*, *ibid.* **371**, 503 (1994).
3. G. Bond *et al.*, *ibid.* **365**, 143 (1993).
4. K. Sakai and W. R. Peltier, *J. Climate* **10**, 949 (1997).
5. U. von Grafenstein, H. Erlenkeuser, J. Müller, P. Trimborn, J. Alets, *Geochim. Cosmochim. Acta* **60**, 4025 (1996).
6. U. von Grafenstein, H. Erlenkeuser, P. Trimborn, *Palaeogeogr. Palaeoclimatol. Palaeoecol.* **148**, 133 (1999).
7. K. Rozanski, L. Araguás-Araguás, R. Gonfiantini, *Science* **258**, 981 (1992).
8. U. Eicher, *Geogr. Helv.* **42**, 99 (1987).
9. T. Goslar, M. Arnold, M. F. Pazdur, *Radiocarbon* **37**, 1 (1995).
10. G. S. Lister, *Quat. Res.* **29**, 129 (1988).
11. A. Schwab, G. S. Lister, K. Kelts, *J. Paleolimnol.* **11**, 3 (1994).
12. D. Hammarlund and B. Buchardt, *Boreas* **25**, 8 (1996).
13. U. von Grafenstein, H. Erlenkeuser, J. Müller, A. Kleinmann-Eisenmann, *Naturwissenschaften* **79**, 145 (1992).

14. U. von Grafenstein, H. Erlenkeuser, A. Kleinmann, J. Müller, P. Trimborn, *J. Paleolimnol.* **11**, 349 (1994).
15. U. von Grafenstein, H. Erlenkeuser, J. Müller, J. Jouzel, S. Johnsen, *Clim. Dyn.* **14**, 73 (1998).
16. A. Brauer, C. Endres, J. F. W. Negendank, *Quat. Int.*, in press; T. Litt and M. Stebich, *ibid.*, in press.
17. S. Joussaume, V. Masson, Paleoclimate Modeling Inter-comparison Project members, personal communication.
18. D. Barber *et al.*, in preparation.
19. D. Klitgaard-Kristensen, H. P. Sejrup, H. Hafliðason, S. Johnsen, M. Spurk, *J. Quat. Sci.* **13**, 165 (1998).
20. S. Björck *et al.*, *Science* **274**, 1155 (1997).
21. L. D. Keigwin and G. A. Jones, *Paleoceanography* **10**, 973 (1995).
22. N. Koc Karpuz and E. Jansen, *ibid.* **7**, 449 (1992).
23. H. Hafliðason, H. P. Sejrup, D. K. Kristensen, S. Johnsen, *Geology* **23**, 1059 (1995).
24. S. J. Johnsen *et al.*, *Medd. Groen. Geosci.* **29**, 1 (1992).
25. Elevation changes of the ice surface at Summit, for example, could have provoked local modifications of $\delta^{18}\text{O}_p$ in addition to regional temperature changes. However, for the period of interest, during deglaciation, such elevation changes give a rise of only $\pm 0.25\%$ [S. J. Johnsen, D. Dahl-Jensen, W. Dansgaard, N. Gundestrup, *Tellus* **47**, 624 (1995)], considerably less than needed to explain the observed transatlantic differences.
26. R. C. Fairbanks, *Nature* **342**, 637 (1989).
27. A. S. Dyke, J. Hooper, J. M. Savelle, *Arctic* **49**, 235 (1996).
28. A. S. Dyke, J. England, E. Reimitt, H. Jetté, *ibid.* **50**, 1 (1997).
29. N. Koç and E. Jansen, *Geology* **22**, 523 (1994).
30. R. B. Alley *et al.*, *Nature* **362**, 527 (1993).
31. G. C. Bond and R. Lott, *Science* **267**, 1005 (1995).
32. D. R. McAyee, *Paleoceanography* **8**, 775 (1993).
33. High-resolution sections were sampled continuously in 1-cm (AS92-5, AS93-1, and below 1218 cm in AS96-1) or 0.5-cm slices (AS96-1, above 1218 cm). If available, up to 30 valves of juvenile *Fabaeformiscandona levanderi* and *Fabaeformiscandona triccricricosa* were used for isotope measurements (Kiel carbonate device on-line-coupled to a Finnigan MAT 251 gas isotope ratio mass spectrometer). For samples smaller than 12 μg of CaCO_3 , a specially designed valve-cold finger gas provider assembly at the gas inlet capillary of the spectrometer (H.-H. Cordt and H. Erlenkeuser, in preparation) was used, which provides reliable measurements for samples as small as 6 μg with an external error of less than 0.08‰ on the $\delta^{18}\text{O}$ scale (1 σ). $\delta^{18}\text{O}_{\text{CS}}$ gives a reliable estimate of the oxygen isotopic composition of former lake water ($\delta^{18}\text{O}_l$) after correction for a vital offset of 2.2‰ (6) and the fractionation between water and calcite at 4°C [I. Friedman and J. R. O'Neil, *U.S. Geol. Surv. Prof. Pap.* **440** (1977)]. The tephra layer from the Laacher See eruption in AS96-1 (LST) is characterized by a strong increase in the magnetic susceptibility, large amount of well-preserved diatom frustules, and rare glass particles in the silt fraction. Geochemical analysis of these particles has not yet been performed. However, the relative position of the layer with respect to the $\delta^{18}\text{O}$ record is the same as for the well-marked LST ash layer in the littoral cores from Ammersee (14) [R. Klee, R. Schmidt, J. Müller, *Limnologia* **23**, 131 (1993)] and from Swiss Lakes (8).
34. We thank H. Heckt and H.-H. Cordt for mass spectrometry and M. Jouzel and L. Osuna for sample preparation. R. Niederreither provided the coring device and with M. Herz assisted during coring. Accelerator mass spectrometry ^{14}C measurements for core AS96-1 were performed by M. Paterne (LSCE) and by G. Bonani and I. Hajdas (Eidgenössische Technische Hochschule-Zürich) for core AS92-5. The manuscript profited from discussion with G. Hoffmann, L. Labeyrie, and M. Elliot and from the reviewers' comments. The GRIP project was financed by the national funding bodies of Belgium, Denmark, France, Germany, Iceland, Italy, Switzerland, and the UK as well as the XII Directorate of the European Union and organized with the support of the European Science foundation.

1 February 1999; accepted 21 April 1999